Korean J. Chem. Eng., 34(3), 600-608 (2017)
DOI: 10.1007/s11814-016-0365-2

pISSN: 0256-1115
eISSN: 1975-7220

REVIEW PAPER

Facile synthesis of imprinted submicroparticles blend polyvinylidene fluoride membranes at ambient temperature for selective adsorption of methyl *p*-hydroxybenzoate

Yanhua Cui, Minjia Meng, Dongshu Sun, Yan Liu, Jianming Pan, Xiaohui Dai, and Yongsheng Yan†

School of Chemistry and Chemical Engineering, Jiangsu University, Zhenjiang 212013, China
(*Received 1 July 2016 • accepted 27 December 2016*)

Abstract−We developed a simple phase inversion technique to prepare molecularly imprinted membrane (MIM) at room temperature for membrane selective adsorption and separation of methyl *p*-hydroxybenzoate (M4HB). The prepared SMIP-MIM was characterized by SEM, FT-IR, TGA. Compared with non-imprinted membrane ($NIM_{1\text{-}5}$) adsorbent, SMIP-$MIM_{1\text{-}5}$ adsorbent with high specific surface area and showed higher binding capacity, faster kinetic and better selectively adsorption capacity for M4HB. The maximum isotherm adsorption capacity for M4HB of SMIP-MIM_4 was 3.519 $mg \cdot g^{-1}$, and the experimental data was well fitted to the slips model by multiple analysis. The maximum kinetic adsorption capacity and equilibrium adsorption time for SMIP-MIM_4 were 1.335 $mg \cdot g^{-1}$ and 160 min, respectively. The mechanism for dynamic adsorption of M4HB onto SMIP-MIM_4 was found to follow pseudo-first-order model and pseudo-second-order model. Additionally, the permeability separation factor of SMIP-MIM_4 for M4HB compared to a structural analogues methyl 2-hydroxybenzoate (M2HB) could reach 2.847. The adsorption capacity of SMIP-MIM_4 for M4HB and M2HB was 0.549 $mg \cdot cm^{-2}$ and 1.563 $mg \cdot cm^{-2}$, respectively. The adsorption behavior of M4HB through SMIP-MIM_4 followed the retarded permeation mechanism.

Keywords: Methyl *p*-Hydroxybenzoate, Molecular Imprinted Membranes, Selective Adsorption, Phase Inversion Technique

INTRODUCTION

To prevent deterioration, various additives and preservatives are applied in medicines, food products and cosmetics. Methyl *p*-hydroxybenzoate (M4HB) as a useful preservative is frequently applied in organic synthesis, cosmetics, medicine, food products and pharmaceuticals due to its lower toxicity, no irritation and suitability for a wide range of PH [1,2]. However, allergic reactions have occurred when products contain methyl *p*-hydroxybenzoate. Besides, it has been shown that long-term use of M4HB products can lead to skin aging, DNA damage and disorder endocrine trigger cancer in current studies [3,4]. What is more, M4HB as a methyl ester of *p*-hydroxybenzoic is generally applied in beverages and some canned foods. So, it is continually discharged into the environment through domestic wastewater and food chains for a long time [5]. Therefore, there is no doubt that it is significant and essential to absorb M4HB and to make sure that the concentration of M4HB in cosmetics and food is lower than the limit set by the state level. But the challenge is that it is difficult through the traditional technologies to selectively separate M4HB due to very low content of analysis product, such as distillation, high-performance liquid chromatography, liquid-phase, extraction and adsorption. Among these processes, adsorption is an economically feasible and efficient method for separating M4HB. However, the direct analysis of M4HB is often disturbed because of its homologous series including methyl, ethyl, butyl, heptyl, and benzyl *p*-hydroxybenzoic in the environmental samples [2]. Absorption always cannot effectively separate M4HB with a relative low concentration for its poor selectivity. Therefore, it is important to develop a simple and highly effective method to separate M4HB from complex samples.

Molecular imprinting technique (MIT) has been used worldwide to separate the specific target molecules. Molecular imprinting technology uses the target molecule as a template; the monomers and cross-linking agent under certain condition polymerization reaction, and then the target molecular eluted, eventually form molecularly imprinted polymers (MIPs) with similar spatial structure to target molecules and specific binding sites toward analytes. MIPs have some outstanding advantages in selectively separating, low-cost, high thermal and chemical/mechanical stability [6-9]. We previously investigated the effect of submicrosized molecularly imprinted polymer on silica submicroparticles for highly selective absorption of M4HB [5]. However, it also has several drawbacks; common MIPs are not beneficial to be separated from samples and difficult to recycle from other situations. Furthermore, the small MIPs still reserve in the treated water, which can cause new environmental pollution problems [10-12]. To effectively overcome these obstacles, it is a challenging task to develop a novel and efficient method for the selective separation of M4HB. So far, some MIPs have been grafted on a matrix such as polypropylene non-woven fabric or polymer membranes [13-15].

Recently, molecularly imprinted membrane (MIM) has become one of the research hotspots that is attracting tremendous interest

†To whom correspondence should be addressed.
E-mail: yanyongsheng66@163.com

in the separation area [16]. MIM is an emerging technology including both the advantages of molecular imprinting technology and membrane separation technology. The basic mechanism behind molecular imprinting is the interaction between the molecules binding sites of polymer matrix and the template molecule through physicochemical and chemical methods [6]. Therefore, MIM is capable to provide the membrane with specific selectivity for separating template molecules by simple membrane permeation process [17]. MIM is the result of combining MIP which bears favorable molecular selectivity, specific separation performance, integrity, stability, less energy consumption, remarkable mechanical properties, fast binding kinetics and continuously separating mixtures. Besides, MIM can be removed easily and is beneficial for the effective recycling of valuable materials after treatment. Thus, we consider MIM with selective adsorption and separation capability will be a better alternative to MIP for separating M4HB.

Different MIMs demonstrating selectively recognition properties have been fabricated [18]. Phase inversion is a promising method to synthesize flexible and thin membranes with high selectivity to the targeted molecules due to the high efficiency, simplicity and operating at atmospheric pressure of these processes [19-23]. More recently, poly(vinylidene fluoride) (PVDF) used as a membrane material has been extensively applied in phase inversion because of its excellent chemical compatibility in most used organic solvents and its thermal stability, physical robustness and filtration performance. These satisfactory performances have spurred interest in numerous researches on PVDF membrane production and applications [24-26]. However, the application of pure PVDF membrane has been limited because of the extremely hydrophobicity and low permeation property. Therefore, developing a PVDF membrane with excellent hydrophilic performance and high selectively recognizing property is extremely significant. So far, several researches have been devoted to improve hydrophilicity of PVDF membranes, including using hydrophilic polymers additives such as poly(ethtylene glycol) (PEG) and polyvinylpyrrolidone (PVP), showing specific affinity toward a target molecule. Uragami et al. [27] prepared PVDF hollow fiber membranes with different porosity and pore size by adding PEG to improve the PVDF membrane permeability and hydrophilicity. Moghareh Abed et al. [28] prepared PVDF-g-POEM membrane via atom transfer radical polymerization (ATRP) and observed the morphology, physical properties, permeability of membranes; it showed that the hydrophilicity of the membrane surface was improved. To our knowledge, there are few researches on selective separation M4HB using submicrosized imprinted membranes as adsorbents to improve their adsorption behavior.

Therefore, our objective here was to present a simple and environment friendly phase-inversion process to prepare a high performance molecularly imprinted membrane for selectively separating M4HB. We used PVDF powder mixed with surface molecularly imprinted microspheres (SMIP) prepared using a sol-gel process dissolved in NMP as a casting solution. Tetraethox-ysilane (TEOS) and aminopropyltriethoxysilane (APTES) were chosen as cross-linker and functional monomer, respectively. Using silica submicroparticles as the support was because it is a simple, available and potential imprinting material to improve imprinting effect. The so-prepared SMIP-MIM was then characterized and successfully applied in the practical application about adsorption of target object (M4HB) in the aqueous solution. And the imprinting efficiency selectivity of SMIP-MIM/NIM was also evaluated by te batch mode experiments. The selectivity of the prepared membrane was investigated over competitive compounds, and the results showed that the SMIP-MIM was capable to selectively adsorb M4HB.

EXPERIMENTAL

1. Instruments and Materials

1-1. Equipment and Instruments

In this study, so-applied apparatuses were as follows: Fourier transform infrared (FTIR) spectrometer with the wave number range of 4,000-400 cm^{-1} was recorded on a Nicolet NEXUS-470 FT-IR instrument (USA). Thermal gravimetry analysis (TGA) curves of samples were obtained by using a thermoanalysis instrument (NETZSCH STA 449C) in 10 $^{o}C \cdot min^{-1}$ under the condition of heating rate. The morphologies of the samples were studied by scanning electron microscopy (SEM, S-4800).

1-2. Materials and Reagents

Polyvinylidene fluoride (PVDF Mn¼110,000 $g \cdot mol^{-1}$, Solef 6010) was provided by Solvay Solexis (Changshu, China). N-methyl pyrrolidone (NMP) was purchased from Sinopharm Chemical Reagent (Shanghai, China). Methyl 2-hydroxybenzoate (M2HB), methyl *p*-hydroxybenzoate (M4HB), Tetraethoxysilane (TEOS), Ammonium Hydroxide ($NH_3 \cdot H_2O$, 25-28%) and aminopropyltriethoxysilane (APTES) were all bought from Aladdin Chemistry (Shanghai, China). All other reagents used in this experiment were analytical and purchased by commercial channels. Ultrapure water used throughout the experiments was obtained from an in-house laboratory purification system.

2. Synthesis and Characterizations of SMIP-MIM

2-1. Preparation of the Silica Microspheres

2.0 mL of $NH_3 \cdot H_2O$, 5.0 mL distilled water and 14 mL anhydrous ethanol absolute were initially mixed to obtain solution A, then 1.0 mL of TEOS and 25 mL anhydrous ethanol absolute were mixed to obtain solution B. Under magnetic stirring conditions, solution B was slowly poured into solution A for 1.0 min, then the stirring speed variable was adjusted to 300 rpm, with continuous stirring for 4.0 h to form white silica colloidal suspension; finally through centrifugal separation of the suspension and the product was precipitated in anhydrous ethanol and washed for three times with ultrapure water. The so-obtained product was centrifuged and dried to obtain silica microspheres.

2-2. Preparation of the Surface Molecularly Imprinted Submicroparticles

The surface molecularly imprinted submicroparticles were prepared using a sol-gel process according to the report by Meng [29] et al. In a typical experiment, 1.87 mL of APTES (8.0 mmol) and 0.304 g of M4HB (2.0 mmol) were added into 400 mg silica submicroparticles which were dissolved in 20 mL of methanol for 2.0 h under ultrasonic vibration conditions to obtain the absolutely self-assembled composites with M4HB. Then, 1.0 mL of HAc (1.0 $mol \cdot L^{-1}$) and 3.0 mL of TEOS (7.56 mmol) were added into the above suspension under magnetic stirring at 300 rpm for 18 h to form particles with a high precise cross-linking structure. The obtained

polymer was then washed with 100 mL of a mixture of methanol and 6 mol·L^{-1} HCl (1 : 1, V/V) for three times and neutralized with ultrapure water to remove M4HB. Finally, the polymer was dried at 60 °C for 12 h to obtain the surface molecularly imprinted microspheres.

2-3. Fabrication of SMIP-MIM

The molecularly imprinted membranes were prepared using phase inversion technique according to the report by Zhang [30] et al. 0.05 g (or 0.10 g, 0.15 g, 0.20 g, 0.25 g) of SMIP were added into 0.5 g of PVDF powders, which were dissolved into 9.5 mL of NMP under stirring at 300 rpm; then 0.2 mL of ammonia solution was added into the above solution under continuous stirring for 6 h to obtain transparent solution. After stewing to exhaust the air bubbles, the casting solutions were transferred on a smooth and clean glass plate under room temperature, then 30 s later the glass plate was promptly immersed into the deionized water bath to perform phase inversion to obtain the PVDF membrane (SMIP-MIM_1 or SMIP-MIM_2, SMIP-MIM_3, SMIP-MIM_4, SMIP-MIM_5), and the process began between the distilled water and the polymers. Finally, the membrane sheets were washed by deionized water for three times to totally remove the residual NMP. Before tests the imprinted membranes were stored in deionized water.

The corresponding nonimprinted membrane (NIM_{1-5}) preparation and treatment method is the same as above but without template M4HB.

2-4. Static Adsorption Experiments

The adsorption static experiments were carried out to study the effect of the content of SMIP in SMIP-MIMs for the adsorption capacity of SMIP-MIMs. 0.02 g of SMIP-MIM_{1-5} was added into the numbers of 10 mL of M4HB solutions that the solvent was methanol/water (3/7, V/V) [31,32] with concentrations 20 mg·L^{-1}, respectively. These compounds were shaken on a constant temperature shaker at 25 °C, and after 4 h the residual concentrations of M4HB in the supernatants were determined with UV spectrophotometry at the wavelength of 256 nm, respectively. The adsorption amounts (Q_e, mg·g^{-1}) [33] were calculated by the following:

$$Q_e = \frac{(C_0 - C_e)V}{m} \quad (1)$$

where C_0 (mg·L^{-1}) and C_e (mg·L^{-1}) are the initial and equilibrium concentrations of M4HB, respectively. V (mL) and m (g) are the volume of the solution and the weight of the membrane, respectively.

2-5. Kinetics Adsorption Experiments

In the adsorption kinetics experiments, 0.02 g of SMIP-MIM_{1-5} were accurately taken into a 10.0 mL centrifuge tube and then 20.0 mL of M4HB water solutions (200 mg·L^{-1}) were added. These mixtures were shaken on a constant temperature shaker. After an interval of time, the residual concentrations of M4HB in mixed solutions were obtained and determined using UV at a wavelength of 256 nm, respectively. The binding amounts (Q_t, mg·g^{-1}) [34] were determined by the following Q_t, and the time of adsorption equilibrium was obtained.

$$Q_t = \frac{(C_0 - C_t)V}{m} \quad (2)$$

where C_0 and C_t (mg·L^{-1}) are the feed concentration at the initial time and the sampling time, respectively. V and m are the volume of the solution (mL) and weight of the prepared membrane (g), respectively.

2-6. Isotherm Adsorption Experiments

The adsorption isotherm of M4HB was performed in 10 mL centrifuge tubes by the addition 0.02 g of SMIP-MIM or SMIP-NIM into 9.0 mL M4HB water solution with different concentrations ranging from 20 mg·L^{-1} to 280 mg·L^{-1} at room temperature. After 4.0 h of stewing, the residual concentration of M4HB in the mixed solution was determined using UV absorption spectroscopy at a wave length of 256 nm. The equilibrium binding amounts were calculated (Q_e, mg·g^{-1}) by the following:

$$Q_e = \frac{(C_0 - C_e)V}{m} \quad (3)$$

where C_0 (mg·L^{-1}) and C_e (mg·L^{-1}) are the initial and equilibrium concentrations of M4HB, respectively. V (mL) and m (g) are the volume of the solution and the weight of the membrane, respectively.

2-7. Permeation Experiments

Permeation experiments were carried out for M4HB to investigate the selective permeation of SMIP-MIM and SMIP-NIM that was evaluated toward competitive substrates M4HB and M2HB using the mixture solutions containing 100 mg·L^{-1} of M4HB and M2HB as the feeding solution in H-model tube installation (Fig. 1). The volume of each chamber was 150 mL, while the membrane, with an effective cross-section area of 1.5 cm^2, was fixed tightly between two text chambers of a permeation cell. The mixture solution of M4HB and M2HB (100 mL) of 100 mg·L^{-1} in methanol/water (3 : 7, V/V) media was placed in the left-hand side chamber, while 100 mL blank methanol/water (3 : 7, V/V) was placed in the right-hand side chamber. In both chambers, solutions were kept homogeneous by the magnetic stirrer at 25 °C. Finally, the concentration of both M4HB and M2HB in the permeate solution obtained from the left-hand side solution was determined by UV system at different points of sampling time. A volume of blank methanol/water (3 : 7, V/V) was added into the left-hand side chamber to maintain a constant volume. The solute permeation amounts Q_{pt} (mg·cm^{-2}) [35] were calculated by the following:

$$Q_{pt} = \frac{C_t V}{A} \quad (4)$$

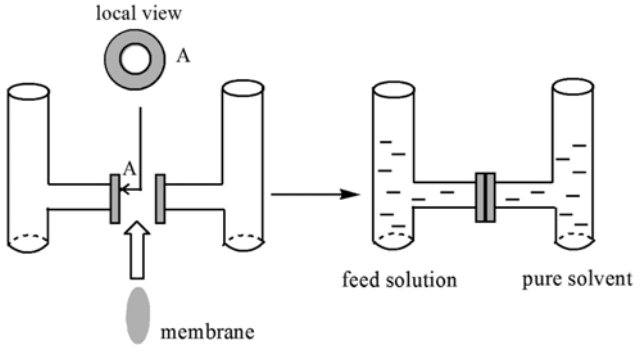

Fig. 1. Diagram of H-shaped two-compartment cell permeation installation.

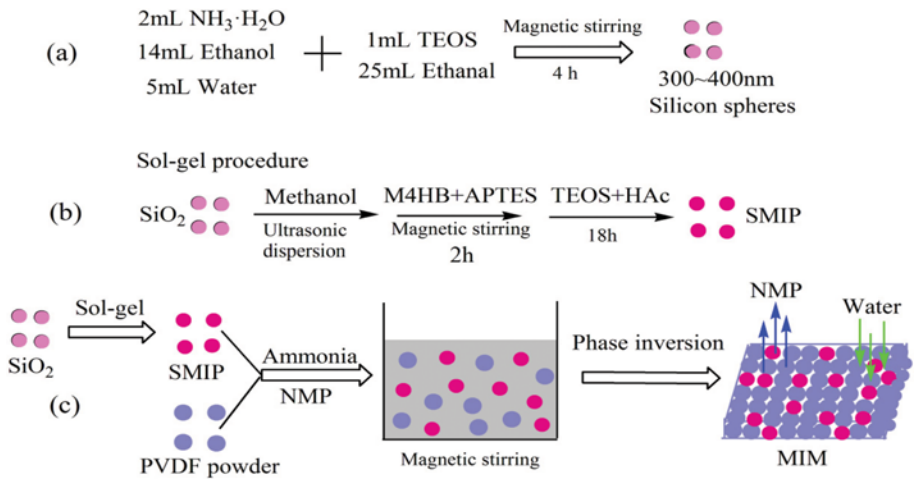

Fig. 2. Schematic diagram of the synthesis of molecularly imprinted membrane.

where C_t (mg·L^{-1}) is the concentration of permeation molecules at any time, V (L) and A (cm^2) are the volume of the solution and the effective cross-section area of the membrane, respectively.

To evaluate the permeation special selectivity of the obtained membranes, a separation factor (ap) was chosen as a parameter β, which was defined as the ratio of the average permeation amount of M4HB and M2HB. The permeation special selectivity amounts β were calculated by the following:

$$\beta = \frac{Q_p M2HB}{Q_p M4HB} \quad (5)$$

where Q_{pM2HB} and Q_{pM4HB} (mg·cm^{-2}) are the permeation amounts of competitive substrate and template molecular, respectively, at the final time.

RESULTS AND DISCUSSION

1. Preparation of SMIP-MIM

The whole fabrication procedure of molecular imprinted membrane contained three steps as shown in Fig. 2. In the first step (a), the particle size of silica microspheres was determined by the additional amount of TEOS, and the more of TEOS that was added, the larger the particle size of silica microspheres became. Reducing the content of TEOS to prepare silica microspheres would increase the difficulty of separating the particles from the solution, which required the speed of centrifugation should be kept extremely high and the time of centrifugation should be kept longer even, and the product rate was also not high. The mechanical strength of the silica microspheres was influenced by the time of mechanical stirring; the shape of silica microspheres could become oval after a slight squeeze with short time as one or two hours, while the shape of silica microspheres could form spheres and hardly deform after three or four hours. That was because the structure of the microspheres was loose in the early growth of core-shell, and with the increase of time it would become increasingly tight. In the second step (b), APTES was not only as a medium for connecting silica microspheres, but also as a functional monomer with target molecular M4HB forming self-assembling compound, wherein the acetic acid and TEOS acted as catalyst and cross-linking, respectively. The key step in the preparation was agent neutralization. Only when the template molecule in the polymer was completely removed and kept neutral can SMIP show the most excellent adsorption performance. In the third step (c), adding ammonium hydroxide for producing dehydrofluorination reaction made the polymer chains cross-linked and improved the mechanical properties of membranes.

2. Characterizations

FT-IR technique was used to examine the changes in chemical structures. The FTIR spectra of (a) SMIP and (b) SMIP-MIM$_4$ are shown in Fig. 3. As shown in Fig. 3(a) and (b), the absorption peak at 468 cm^{-1} was attributed to the bending vibration characteristic peak of Si-O-Si. In addition, the broad band observed around 2,900 cm^{-1} was ascribed to the stretching vibration of N-H of the amino, indicating that APTES was successfully grafted to the surface of silica microspheres. As shown in Fig. 3(b), the absorption band at 1,182 cm^{-1} was assigned to stretching vibration of C-F of PVDF, and in (b), the absorption peaks at 468 cm^{-1} and 2,900 cm^{-1}

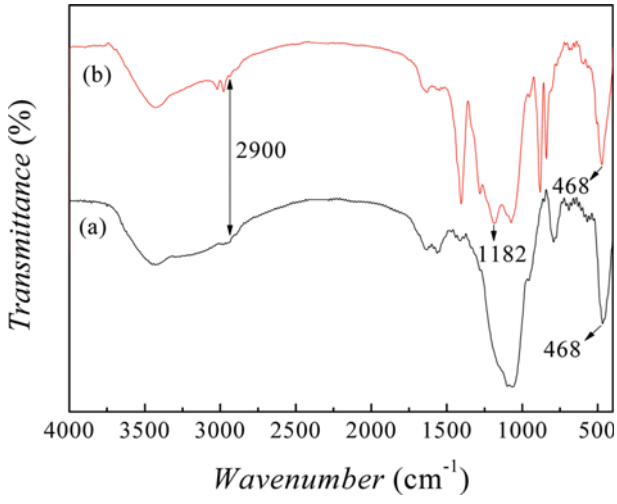

Fig. 3. FTIR of SMIP (a) and SMIP-MIM$_4$ (b).

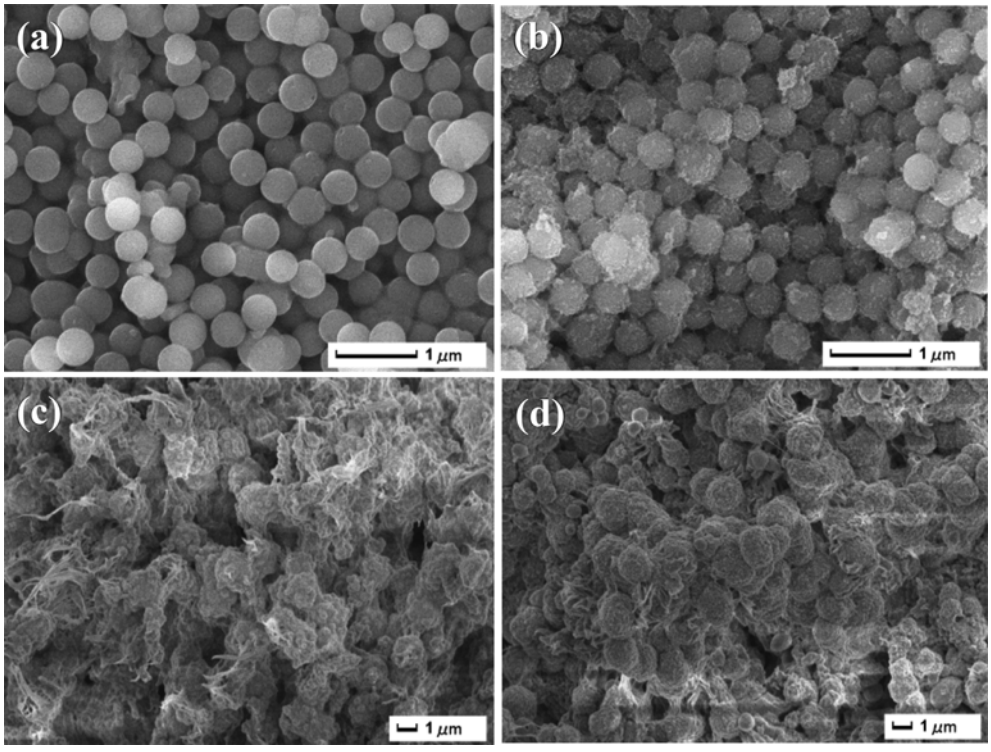

Fig. 4. SEM of SiO_2 (a), SMIP (b), PVDF membrane (c), SMIP-MIM_4 (d).

were attributed to the bending vibration characteristic peak of Si-O-Si and the stretching vibration of N-H of the amino, respectively, illustrating that the surface molecular imprinting microsphere had been integrated into the PVDF membrane. The result of FTIR indicated that the SMIP-MIM was prepared successfully.

The morphologies of the SiO_2, SMIP, PVDF membrane and SMIP-MIM_4 are shown in Fig. 4. In Fig. 4(a) silica particles display uniform shape and particle size around 300 nm with a smooth surface. However, in Fig. 4(b), the surface of microspheres became rough, but particle size did not obviously increase, which indicated that the molecularly imprinted polymer layer was successfully grafted on the surface of silica microspheres. As shown in Fig. 4(c), PVDF microspheres were connected by filaments combined into a membrane. In Fig. 4(d), SMIP particles were embedded between PVDF microspheres bearing certain pore. The result of (SEM) indicated that the SMIP-MIM was prepared successfully.

TGA was used to detect thermal stability and the degradation behavior of SMIP-MIM_4, PVDF membrane and SMIP. The resulting TGA curves of SMIP-MIM_4, PVDF membrane and SMIP are shown in Fig. 5. As depicted in Fig. 5, it was found that with the increasing of temperature initially, the quality of SMIP-MIM_4 and PVDF membrane slightly dropped, this was mainly on account of the presence of an amount of the physically absorbed water molecules of membranes. SMIP-MIM_4 and PVDF membrane presented slightly higher loss of about 66.37% and 58.54% with the temperature increasing and the speed of membrane quality reduced quickly, this was mainly due to producing dehydrofluorination reaction of the PVDF membrane which leaded to mass loss. With the temperature increasing, the mass loss of SMIP-MIM_4 changed more

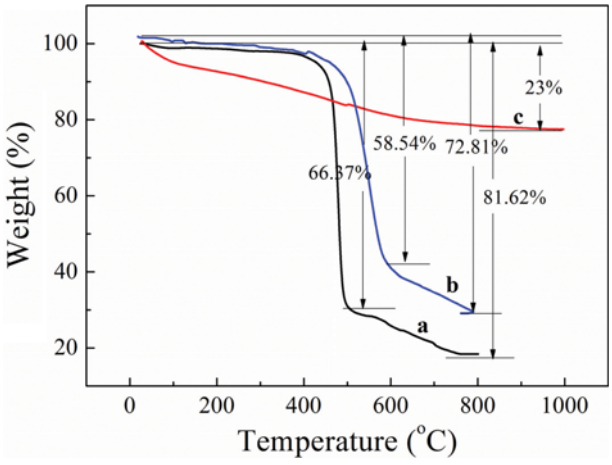

Fig. 5. TGA curves of (a) SMIP-MIM_4 (b) PVDF membrane and (c) SMIP.

slowly, finally maintained unchanged, the weight of the remaining 18.38% was the amount of SiO_2 that posed thermal stability. In addition, SMIP had a slight weight loss of about 23% from room temperature to 1,000 °C, regarding the loss of absorbed water and the floccules-like imprinting coating present on the surface of silica submicroparticles during the process of imprinting.

3. Effect of the Content of SMIP

The experiment was made with five kinds of SMIP-MIM and the difference of which was that the amount of SMIP in each SMIP-MIM was different; the ratio of SMIP content and the additional amount of PVDF in SMIP-$MIM_{1\text{-}5}$ was 10%, 20%, 30%, 40% and

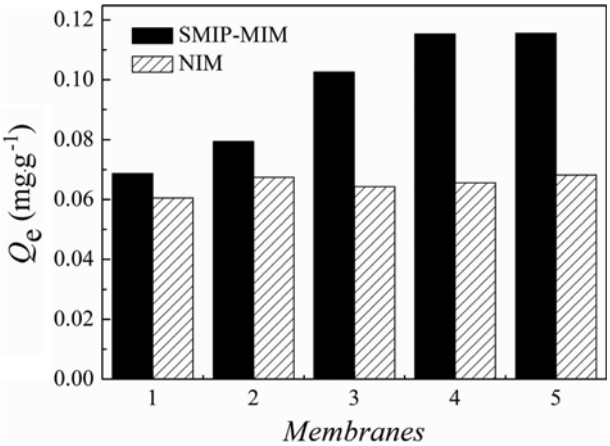

Fig. 6. Adsorption capacity of SMIP-MIM$_{1\text{-}5}$ and NIM$_{1\text{-}5}$.

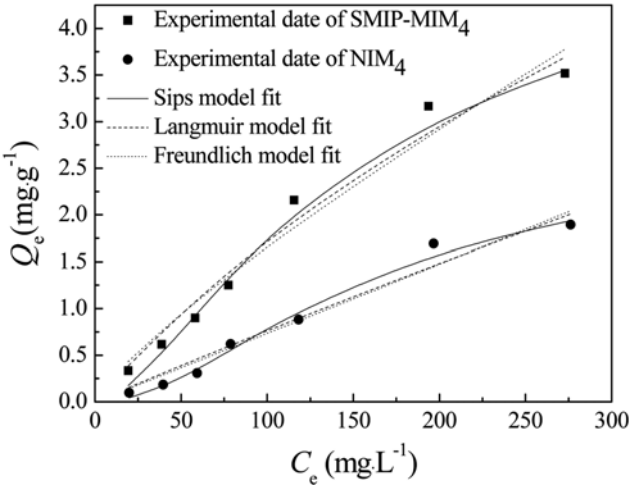

Fig. 7. Equilibrium experimental data and modeling fit for the adsorption of M4HB onto SMIP-MIM$_4$ and NIM$_4$.

50%, respectively. The adsorption capacity of the membrane was evaluated by static adsorption experiments, and the results are shown in Fig. 6. As one can see from the figure, the adsorption capacity of SMIP-MIM was obviously increased with the increase of SMIP content; however, the amount of SMIP-MIM$_5$ adsorption was not increased compared with SMIP-MIM$_4$. This was due to the dispersion of certain recognition sites in the inner of the imprinted membrane leading to the M4HB molecule not reaching inside. Furthermore, the adsorption capacity of the nonimprinted membrane NIM$_{1\text{-}5}$ was not obviously affected because of the additional accounts of the nonimprinted microspheres that were kept at the same level and less than the amount of SMIP-MIM adsorption. It was more confirmed that adding SMIP increased the adsorption capacity of the membrane; on the other hand, further adding the amount of SMIP more may reduce the overall mechanical properties of the membrane. So we concluded that the amount of SMIP was not too much and SMIP-MIM$_4$ looked like the experiment objective in this work.

4. Adsorption Isotherm Experiments

The adsorption isotherm experiments were carried out to evaluate the binding performance of the adsorption behavior on the membrane for M4HB. Three isotherm equations widely applied, namely Langmuir, Freundlich and Langmuir-Freundlich (Sips), have been adopted in this study. The Langmuir equation, which is all the binding sites with the same energy and is efficient adsorption onto surface with a limited number of uniform sites [36], is given by Eq. (6).

$$Q_e = \frac{Q_m K_L C_e}{1 + K_L C_e} \tag{6}$$

where Q_e (mg·g^{-1}) is the equilibrium capacity of adsorbed M4HB and Q_m (mg·g^{-1}) is the maximum adsorption amount, C_e (mg·L^{-1}) is the equilibrium concentration of adsorbed M4HB, K_L (L·mg^{-1}) represents the Langmuir affinity constant.

The Freundlich isothermal model assumes that the all the adsorption sites have different energy and occur onto an inhomogeneous surface [37]. The nonlinear expression of the model is:

$$Q_e = K_F C_e^{1/n} \tag{7}$$

where K_F (mg·g^{-1}) is the adsorption isothermal constant of the Freundlich model, 1/n expresses a degree or commutative of the strength inhomogeneous. If the 1/n value is less than 1.0, it means that it is beneficial for removal conditions [38].

Langmuir-Freundlich (Sips) is Freundlich power-law tables introduced on the base of the Langmuir isotherm equation [39]; the equations as follows:

$$Q_e = \frac{Q_m K_s (C_e)^{ns}}{1 + K_s (C_e)^{ns}} \tag{8}$$

where the K_s [(L·mg^{-1})^{ns}] is the Sips adsorption isothermal constant, representing the adsorption capacity, n_s is the empirical constant.

The equilibrium adsorption values with different concentrations of imprinted membrane and nonimprinted membrane are shown in Fig. 7. As seen, the adsorption values of SMIP-MIM$_4$ and NIM$_4$ on M4HB increased with the increase of concentration of M4HB, and the adsorption capacity was roughly the same. It was different that at the same concentration, the adsorption capacity of the former was much higher than that of the latter and in the concentration range of the experiment the maximum adsorption capac-

Table 1. Adsorption equilibrium parameters for Langmuir, Freundlich and Sips isotherm equations

Sample membrane	Langmuir			Freundlich			Sips			
	Q_m (mg·g^{-1})	K_L (L·mg^{-1})	R^2	K_F (mg·g^{-1})	1/n	R^2	Q_m (mg·g^{-1})	K_S [(L·mg^{-1})^{ns}]	n_s	R^2
SMIP-MM$_4$	10.77	1.9×10^{-3}	0.974	0.038	0.818	0.960	4.575	2.8×10^{-4}	1.674	0.989
NIM$_4$	27.33	2.8×10^{-4}	0.958	0.007	1.006	0.958	2.460	4.1×10^{-5}	2.017	0.987

ity of SMIP-MIM_4 and NIM_4 were 3.519 mg·g^{-1} and 1.897 mg·g^{-1}, respectively. Three kinds of models fitting the curves of the isothermal experimental data are also presented in Fig. 7, the so-fitted relevant parameters are shown in Table 1. From the graph, the model of the fitting curve or through the contrast table in the correlation coefficient R^2 value (above 0.98) can be found that the Sips model was a fit to the experimental data than the other two models, predicting the largest adsorption capacity for SMIP-MIM_4 and NIM_4 through the model was 4.575 mg·g^{-1} and 2.460 mg·g^{-1}, approaching to the adsorption amount of SMIP-MIM_4 and NIM_4 for M4HB. This stated that a inhomogeneous membrane surface but had certain amount of energy of the adsorption sites.

5. Adsorption Kinetics Experiments

The adsorption rate is a significant characteristic and parameter used to reflect the adsorption procedure. To further investigate the effects of template molecular M4HB on the adsorption behavior of SMIP-MIM and SMIP-NIM, two typical kinetic models were applied to analyze the binding process: Lagergren pseudo-first-order (Eq. (9)) and pseudo-second-order model (Eq. (10)) [40,41], respectively.

$$Q_t = Q_e(1 - e^{-k_1 t}) \tag{9}$$

$$Q_t = \frac{k_2 Q_e^2 t}{1 + k_2 Q_e t} \tag{10}$$

where Q_t (mg·g^{-1}) and Q_e (mg·g^{-1}) are the adsorption capacity for M4HB of SMIP-MIM and SMIP-NIM at special and equilibrium time t (min), respectively. k_1 (min^{-1}) and k_2 (g·mg^{-1}·min^{-1}) are pseudo-first-order and pseudo-second-order rate constant of equilibrium adsorption, respectively. In accordance with pseudo-second-order rate constant of equilibrium adsorption the initial rate of adsorption h (mg·g^{-1}·min^{-1}) and semi-equilibrium time $t^{1/2}$ (min) [42] can be calculated:

$$h = k_2 Q_e^2 \tag{11}$$

$$t_{1/2} = 1/(k_2 Q_e) \tag{12}$$

In this study, the dynamic adsorption amounts of SMIP-MIM_4 and SMIP- NIM_4 for the template M4HB which ranged with time are shown in Fig. 8. As seen, the dynamic adsorption of SMIP-MIM_4 and SMIP-NIM_4 for M4HB experienced two steps: adsorption quickly and saturation slowly. The adsorption amounts of SMIP-MIM_4 and SMIP- NIM_4 increased quickly with the time before 160 min and then the maximal adsorption amount of SMIP-MIM_4 was up to 0.3 mg·g^{-1} (SMIP-MIM_4); nevertheless, the maximal adsorption amounts of SMIP-MIM_4 and SMIP-NIM_4 reached 94.08% and 90.39% during 160 min, and about 560 min later, the adsorption amounts of two membranes increased slowly and reached equilibrium.

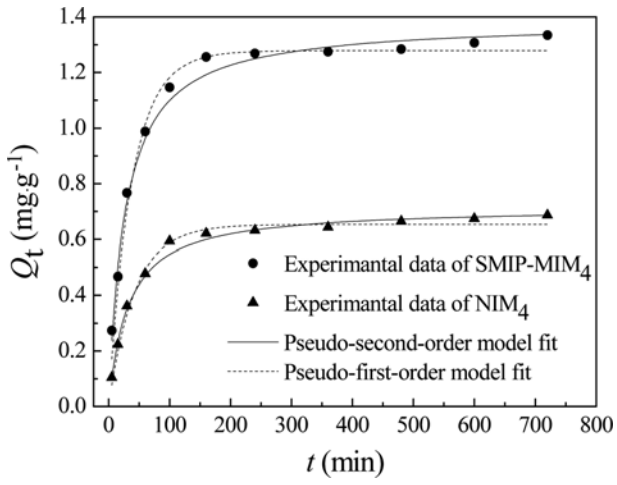

Fig. 8. Kinetic data and modeling fit for the adsorption of M4HB onto SMIP-MIM_4 and NIM_4.

Fig. 8 also presents the nonlinear regression plots of two typical kinetic models of SMIP-MIM_4 and SMIP-NIM_4 for M4HB; the correlation coefficient (R^2) was used to estimate the feasibility of the kinetic models, as shown in Table 2, the correlation coefficient (R^2) (R^2 values above 0.99) of the adsorption procedure by pseudo-second-order kinetic model were higher than that by pseudo-first-order model. In addition, the theoretical values ($Q_{e,cal}$) of equilibrium adsorption of SMIP-MIM_4 and SMIP-NIM_4 calculated by pseudo-second-order were 1.382 mg·g^{-1} and 0.713 mg·g^{-1} which were approximately to the experimental values ($Q_{e,exp}$) that were 1.335 mg·g^{-1} and 0.687 mg·g^{-1}, respectively. Hence, the adsorption behavior of M4HB on SMIP-MIM_4 and SMIP-NIM_4 better followed pseudo-second-order model, and this adsorption process was for the rate control step [43]. Furthermore, the adsorption rate of SMIP-MIM_4 was quicker than of NIM_4 by contrast, showing that the SMIP-MIM_4 was easier for the binding of M4HB. It was observed that imprinted membranes exposed more binding sites and enhanced their adsorption capacity.

6. Permeation Performance

Permeation experiments were carried out for the template molecule (M4HB) and completing molecule (M2HB) extremely to examine the selective permeation of SMIP-MIM and SMIP-NIM. As shown in Fig. 9, the results suggested that the permeation accounts of the template molecule (M4HB) and the completing molecule (M2HB) increased with the time, but the completing molecule (M2HB) showed higher permeation rate than the template molecule (M4HB); the gap between the permeation accounts was directly proportional to the time, so the increase in one variable caused a change in the other, the permeation amounts of M4HB

Table 2. Kinetic parameters for the pseudo-first-order and pseudo-second-order equations

Sample membrane	$Q_{e,exp}$ (mg·g^{-1})	Pseudo-first-order model			Pseudo-second-order model				
		$Q_{e,cal}$ (mg·g^{-1})	k_1 (min^{-1})	R^2	$Q_{e,cal}$ (mg·g^{-1})	K_2 (g·mg^{-1}·min^{-1})	h (mg·g^{-1}·min^{-1})	$T_{1/2}$ (min)	R^2
SMIP-MIM_4	1.335	1.279	0.029	0.981	1.382	0.030	0.057	24.085	0.991
NIM_4	0.687	0.654	0.025	0.987	0.713	0.049	0.025	28.662	0.992

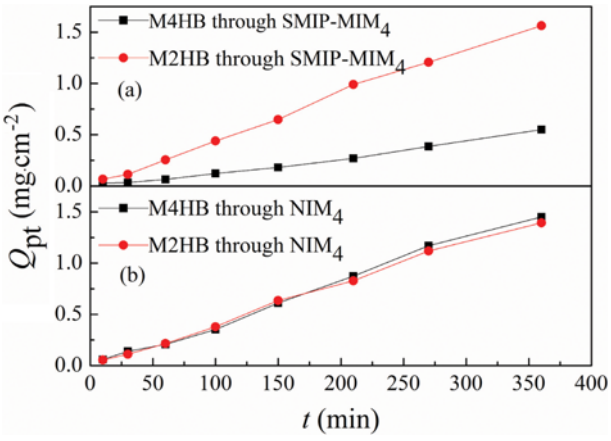

Fig. 9. Time-permeation curves of M4HB and M2HB through the SMIP-MIM$_4$ (a) and NIM$_4$ (b).

and M2HB reached 0.549 mg·cm^{-2} and 1.563 mg·cm^{-2}, respectively, during 360 min, and permeation isolate factor SMIP-MIM4 was up to 2.847. Compared with SMIP-MIM$_4$, diffusion of M4HB and M2HB from the nonimprinted membranes though increased with longer time; the permeation amounts of two membranes were up to 1.451 mg·cm^{-2} and 1.393 mg·cm^{-2} at the same time, respectively, and permeation isolate factor of NIM$_4$ reached 0.960. The results implied the imprinted process improved permeation and separation performance of membranes.

Two major mechanisms applied in analyzing the selective transport could be regarded: (i) facilitated permeation driven by preferential sorption of the template due to affinity binding-slower transport of other solutes, and (ii) retarded permeation due to affinity binding-faster transport of other solutes, until a saturation of imprinted sites with template was reached [44]. Apparently, the behavior of M4HB and M2HB through SMIP-MIM$_4$ followed the retarded permeation mechanism, which indicated that the specific binding sites on the membrane had higher adsorption for M4HB.

CONCLUSIONS

We synthesized molecularly imprinted membrane (SMIP-MIM) with high performance for selectively separating methyl *p*-hydroxybenzoate (M4HB) by the phase inversion technique, using PVDF powder mixed with surface molecularly imprinted microspheres (SMIP) as matrix material. The prepared membrane was characterized by SEM, FT-IR, TGA. The properties of membranes were studied by the bath mode binding and permeation experiments. The static adsorption demonstrated that 0.2 g of SMIP membrane could achieve desirable properties, and compared with non-imprinted membrane (NIM$_{1\text{-}5}$) adsorbent, SMIP-MIM$_{1\text{-}5}$ adsorbent with high specific surface area and showed higher binding capacity, faster kinetic and better selectively adsorption capacity for M4HB. The equilibrium adsorption isotherms of M4HB on SMIP-MIM could be well fitted by the Sips model. The mechanism for dynamic adsorption of M4HB onto SMIP-MIM$_4$ was found to follow pseudo-second-order model. Dynamic binding study demonstrated that the SMIP-MIM had good site accessibility toward M4HB molecules. Additionally, the permeability experiment suggested that SMIP-MIM$_4$ had higher selectivity and better site accessibility for the template M4HB than non-imprinted membrane (NIM$_4$). The SMIP-MIM$_4$ in permeability experiment for M4HB can be better adsorption and separated from the mixture. The adsorption behavior of M4HB through SMIP-MIM$_4$ followed the retarded permeation mechanism. All the aforementioned results indicated the potential application of the SMIP-MIM adsorbents for selectively separation of M4HB in wastewater and food chains treatment. Further, it can be predicted to be applied in the industrial production for the adsorption and separation target analytes in the complex matrix.

ACKNOWLEDGEMENTS

This work was financially supported by the National Natural Science Foundation of China (Nos. U1407123, U1507118, U1507115, 21207051, 21406085), Ph.D. Programs Foundation of Ministry of Education of China (No. 20123227120015), Programs of Senior Talent Foundation of Jiangsu University (No. 15JDG024), Natural science fund for Colleges and Universities in Jiangsu Province (Nos. 15KJB550003, 14KJB150005), China Postdoctoral Science Foundation funded project (2015M581743), Postdoctoral Fund of Jiangsu Province (No. 1501104B) and Natural Science Foundation of Jiangsu Province (Nos. BK20150483, BK2014058).

NOMENCLATURE

Symbols

Q	: adsorbing capacity
A	: area
C	: concentration
R^2	: correlation coefficient
°C	: degree centigrade
g	: gram
h	: hour
L	: litre
m	: mass
mg	: milligram
mL	: milliliter
mmol	: millimole
moL	: moore
Q_{pt}	: permeation capacity
β	: permeation separation factor
V	: volume

Abbreviations

APTES	: aminopropyltriethoxysilane
FT-IR	: fourier infrared spectrum
M4HB	: methyl *p*-hydroxybenzoate
M2HB	: methyl 2-hydroxybenzoate
MIM	: molecularly imprinted membrane
MIPs	: molecularly imprinted polymers
MIT	: molecular imprinting technique
NMP	: N-methyl pyrrolidone
PVDF	: polyvinylidene fluoride

SEM : scanning electron microscopy
SMIP : surface molecularly imprinted microspheres
TEOS : tetraethox-ysilane
TGA : thermal gravity analysis

REFERENCES

1. O. Handa, S. Kokura, S. Adachi, T. Takagi, Y. Naito, T. Tanigawa, N. Yoshida and T. Yoshikawa, *Toxicol.*, **227**, 62 (2006).
2. M. G. Sonia, S. L. Taylorb, N. A. Greenbergc and G. A. Burdocka, *Food Chem. Toxicol.*, **40**, 1335 (2002).
3. Y. Okamoto, T. Hayashi, S. Matsunami, K. Ueda and N. Kojima, *Chem. Res. Toxicol.*, **21**, 1594 (2008).
4. H. Y. Luo, M. Zhang, N. C. Si, M. J. Meng, L. Yan, W. J. Zhu and C. X. Li, *Chin. Chem. Lett.*, **26**, 1036 (2015).
5. M. J. Meng, Z. P. Wang, L. L. Ma, M. Zhang, J. Wang, X. H. Dai and Y. S. Yan, *Ind. Eng. Chem. Res.*, **51**, 14915 (2012).
6. G. Székely, I. B. Valtcheva, J. F. Kim and A. G. Livingston, *React. Funct. Polym.*, **86**, 215 (2015).
7. C. G. Xie, Z. P. Zhang, D. P. Wang, G. J. Guan, D. M. Gao and J. H. Liu, *Anal. Chem.*, **78**, 8339 (2006).
8. M. B. Vazquez and A. D. Spivak, *J. Am. Chem. Soc.*, **126**, 7827 (2004).
9. S. Kazemi, A. A. Sarabi and M. Abdouss, *Korean J. Chem. Eng.*, **33**(11), 3289 (2016).
10. F. Liu, Q. Liu, Y. H. Zhang, Y. J. Liu, Y. C. Wan, K. C. Gao, Y. Huang, W. Xia, H. Y. Wang, Y. Shi, Z. Huang and B. Lu, *Chem. Eng. J.*, **262**, 989 (2015).
11. E. Bektaşoğlu, E. B. Özkütük, A. Ersöz and R. Say, *Korean J. Chem. Eng.*, **32**(8), 1613 (2015).
12. S. Anbalagan, S. K. Ponnusamy, S. R. P. Selvam, A. Sankaranarayan and A. Dutta, *Korean J. Chem. Eng.*, **33**(9), 2716 (2016).
13. K. Y. Zhao, B. B. Lin, W. K. Cui, L. ZH. Feng, T. Chen and J. F. Wei, *Talanta*, **121**, 256 (2014).
14. B. H. Kan, L. ZH. Feng, K. Y. Zhao, J. F. Wei, D. W. Zhu, L. H. Zhang and Q. Ren, *J. Mol. Recognit.*, **29**(3), 115 (2016).
15. K. Y. Zhao, L. ZH. Feng, H. Q. Lin, Y. F. Fu, B. B. Lin,W. K. Cui, S. D. Li and J. F. Wei, *Catal. Today*, **236**, 127 (2014).
16. J. P. Fan, L. Li, Z. Y. Tian, C. F. Xie, F. T. Song, X. H. Zhang and J. H. Zhu, *J. Membr. Sci.*, **467**, 13 (2014).
17. Y. L. Wu, M. Yan, Y. S. Yan, X. L. Liu, M. J. Meng, P. Lv, J. M. Pan, P. W. Huo and C. X. Li, *Langmuir*, **30**, 14789 (2014).
18. Z. H. He, M. J. Meng, L. Yan, W. H. Zhu, F. Q. Sun, Y. S. Yan, Y. Liu and S. J. Liu, *Sep. Purif. Technol.*, **145**, 63 (2015).
19. S. G. Del Blanco, L. Donato and E. Drioli, *Sep. Purif. Technol.*, **87**, 40 (2012).
20. L. Donato, A. Figoli and E. Drioli, *J. Pharm. Biomed. Anal.*, **37**, 1003 (2005).
21. J. Y. Wang, Z. L. Xu, P. Wu and S. J. Yin, *J. Membr. Sci.*, **331**, 84 (2009).
22. R. Kielczynski and M. Bryiak, *Sep. Purif. Technol.*, **41**, 231 (2005).
23. M. H. Lee, T. C. Tsai, J. L. Thomas and H. Y. Lin, *Desalination*, **234**, 126 (2008).
24. L. Donato, F. Tasselli, G. D. Luca, S. G. Del Blanco and E. Drioli, *Sep. Purif. Technol.*, **116**, 184 (2013).
25. S. Nejati, C. Boo, C. O. Osuji and M. Elimelech, *J. Membr. Sci.*, **492**, 355 (2015).
26. R. Moradi, S. M. Monfared, Y. Amini and A. Dastbaz, *Korean J. Chem. Eng.*, **33**(7), 2160 (2016).
27. D. L. Wang, K. Li and W. K. Teo, *J. Membr. Sci.*, **163**, 211 (1999).
28. M. R. Moghareh Abed, S. C. Kumbharkar, A. M. Groth and K. Li, *Sep. Purif. Technol.*, **106**, 47 (2013).
29. M. J. Meng, Z. P. Wang, L. L. Ma, M. Zhang, J. Wang, X. H. Dai and Y. S. Yan, *Ind. Eng. Chem. Res.*, **51**,14915 (2012).
30. W. B. Zhang, Z. Shi, F. Zhang, X. Liu, J. Jin and L. Jiang, *Adv. Mater.*, **25**, 2071 (2013).
31. Zh. H. He, M. J. Meng, L. Yan, W. H. Zhu, F. Q. Sun, Y. Sh. Yan, Y. Liu and S. J. Liu, *Sep. Purif. Technol.*, **145**, 63 (2015).
32. M. J. Meng, Zh. H. He, L. Yan, Y. Sh. Yan, F. Q. Sun, Y. Liu and Sh. J. Liu, *J. Appl. Polym. Sci.*, **132**(42) (2015).
33. A. Bhat, G. B. Megeri, C. Thomas, H. Bhargava, C. Jeevitha, S. Chandrashekar and G. M. Madhu, *J. Environ. Chem. Eng.*, **3**, 30 (2015).
34. D. D. Kavak and S. Ülkü, *Process Biochem.*, **50**, 221 (2015).
35. Y. Q. Zhang, X. Shan and X. Q. Gao, *Sep. Purif. Technol.*, **76**, 337 (2011).
36. M. Mazzotti, *J. Chromatogr. A*, **1126**, 311 (2006).
37. S. J. Allen, G. Mckay and J. F. Porter, *J. Colloid Interface Sci.*, **280**, 322 (2004).
38. H. Y. Zhang, A. M. Li and J. Sun, *Chem. Eng. J.*, **217**, 354 (2013).
39. K. Vijayaraghavan, T. V. N. Padmesh, K. Palanivelub and M. Velan, *J. Hazard. Mater.*, **133**, 304 (2006).
40. Y. S. Ho and G. McKay, *Water Res.*, **33**, 578 (1999).
41. Y. S. Ho and G. McKay, *Process Biochem.*, **34**, 451 (1999).
42. Z. J. Wu, H. Joo and K. Lee, *Chem. Eng. J.*, **11**, 227 (2005).
43. G. Baydemir, M. Andac, N. Bereli, R. Say and A. Denizli, *Ind. Eng. Chem. Res.*, **46**, 2843 (2007).
44. M. Ulbricht, *J. Chromatogr. B.*, **804**, 113 (2004).